Further applications of this technique can include the study of tether dynamics during contact between the tether and the deployer mechanism or guide.

References

[1]Djerassi, S., and Bambeger, H., "Simultaneous Deployment of a Cable from Two Moving Platforms," *Journal of Guidance, Control, and Dynamics*, Vol. 21, No. 2, 1998, pp. 271–276.

[2]Kim, E., and Vadali, S. R., "Modelling Issues Related to Retrieval of Tethered Satellite Systems," *Journal of Guidance, Control, and Dynamics*, Vol. 18, No. 5, 1995, pp. 1169–1176.

[3]Banerjee, Arun K., and Do, Van N., "Deployment of a Cable Connecting a Ship to an Underwater Vehicle," *Journal of Guidance, Control, and Dynamics*, Vol. 17, No. 6, 1994, pp. 1327–1332.

[4]Banerjee, A. K., "Dynamics of Tethered Payloads with Deployment Rate Control," *Journal of Guidance, Control, and Dynamics*, Vol. 13, No. 4, 1990, pp. 759–761.

[5]Blanksby, C., and Trivailo, P., "Deployment/Retrieval, Earth's Magnetic Field Interaction and Tether Severance Modelling for the Tethered Satellite System," *Proceedings of the International Aerospace Congress 1997*, Vol. 1, Sydney, Australia, 1997, pp. 81–96.

Two Projectiles Connected by a Flexible Tether Dropped in the Atmosphere

Geoffrey Frost* and Mark Costello†
Oregon State University, Corvallis, Oregon 97331

Introduction

CONNECTING two bodies by means of a tether has been used in many aerospace applications including tethered spacecraft,[1,2] aircraft air refueling,[3,4] and atmospheric balloons.[5] More recently, designers have proposed weapon systems consisting of two projectiles connected by a tether line.[6] In these concepts the lead projectile is generally a bomb, and the follower projectile is a sensor platform. The ordnance is released from an aircraft at altitude and drops toward a target on the ground. Initially, the two projectiles are rigidly attached. At a prespecified time the projectiles separate and subsequently unreel the tether line. After the tether line is fully payed out, the system settles toward a steady state as it approaches the ground. Maximum tether line loads usually occur shortly after the tether is fully deployed. This time instant is defined as the *snatch* point. Snatch loads are typically large, to the point where line failure is an important concern. Designers must balance the need to unreel the tether line in a specified period of time while at the same time limiting tether line loads, follower projectile acceleration, and lead projectile trajectory deviations. Previous work by Frost and Costello[7] developed a dynamic model suitable for simulating the exterior ballistics of this weapon system from release of the weapon to impact on the ground. Here, we use this dynamic model to establish how primary system design parameters such as projectile mass ratio, drag coefficient ratio, and tether stiffness affect performance of the weapon.

Dynamic Model Description

Both the lead and follower projectiles are modeled as point masses, and the tether line is likewise discretized as an open chain of point masses, or beads, where adjacent mass elements are connected by a spring and damper in parallel. Each bead has three translational degrees of freedom. The projectiles and tether beads are acted upon by gravitational, aerodynamic, and elastic forces. The Earth's surface is used as an inertial reference frame. Air density is computed using the standard atmosphere model.[8] The projectile drag coefficients are Mach-number dependent and are computed by linear interpolation of tabulated data. Aerodynamic forces on the tether line include skin-friction drag along the tether line and flat-plate drag perpendicular to the tether line. As the lead and follower projectiles separate, the tether line pays out. There are two aspects to modeling this process, namely, the pay out of the tether line from the lead projectile and the motion of released tether line. The tether deployment model initially places all tether beads on the lead projectile. As the tether line is payed out, beads are released from the lead projectile into the atmosphere. A bead is not placed into the atmosphere until a sufficient length of line has been unreeled. For this reason, during deployment only a fraction of the tether beads are dynamically active in the atmosphere. When a bead is placed into the atmosphere, it is placed along the line from the release point to the last bead released, and initial conditions are established such that the elastic force across the line is unchanged. This tends to prevent a discontinuity in the tether line out rate as a result of bead release. However, because aerodynamic forces act on the bead immediately after it is released, a slight perturbation is generally observed when a tether bead is released. When a bead is released, the mass of the lead projectile is reduced by the released bead weight; the length from the release point to the last tether bead released is reset along with the stiffness and damping coefficients of the exiting tether line. The elastic force between the lead object and the neighboring bead acts on the reel to pay out the tether line. When the full length of tether line has been unspooled, the acceleration and the velocity of the reel are set to zero.

Simulation Results

Typical values were selected for a generic 2000-lbf (8896.44 N) bomb lead projectile released from a parent aircraft and a follower projectile, which is a sensor platform. The lead projectile is released from the parent aircraft at an altitude of 25,000 ft (7620 m) and a speed of 500 ft/s (152.4 m/s). The lead projectile reference area is 1.77 ft^2 (0.164 m^2). The follower projectile weighs 20 lbf (88.96 N) (1% of the lead projectile) and is released from the lead projectile at $t = 0$ s. The tether line has the following properties: length = 1000 ft (304.8 m), weight per unit length = 0.01 lbf/ft (0.146 N/m), diameter = 0.0082 ft (0.0025 m), stiffness = 62,500 lbf·ft/ft (278,013 N-m/m), skin-friction drag coefficient = 0.007, and flat-plate drag coefficient = 1.1. The tether reel weighs 5 lbf (2.24 N). All simulation results use 100 beads to discretize the tether line.

The separation dynamics are driven in large part by the difference between the drag forces on the lead and follower projectiles. Figure 1 plots the range of the lead and follower projectiles for five different follower-to-lead drag coefficient ratios (1.25, 1.50, 1.75, 2.00, and 5.00). The shape of the drag coefficient curve vs Mach number is identical for both projectiles. As would be expected, a decrease in range is noticed when the drag coefficient ratio is increased. One of the primary questions designers are faced with is how to shape the follower projectile to unreel the tether line over a specified duration of time while at the same time limiting the tether line maximum loads and the follower projectile acceleration at the snatch point. Figure 2 shows the length of tether line deployed from the lead projectile over the trajectory for different drag coefficient ratios. Figure 3 plots the magnitude of the inertial velocity of the lead projectile. When the follower projectile drag coefficient is increased relative to the lead projectile, the tether line pays out more rapidly so that tether line tension acting on the lead projectile is higher over a longer portion of the trajectory, contributing to a decrease in range. For a drag coefficient ratio of 5.0, the decrease in range of 15% is substantial; however, the corresponding decrease in the tether deployment time of approximately 1 s is modest. For the configuration analyzed the steady-state drop velocity is larger than the release velocity so that the lead projectile increases its speed over the trajectory until it impacts the ground and its velocity goes

Received 17 September 1999; revision received 28 May 2000; accepted for publication 20 July 2000.

*Graduate Research Assistant, Department of Mechanical Engineering.

†Assistant Professor, Department of Mechanical Engineering. Member AIAA.

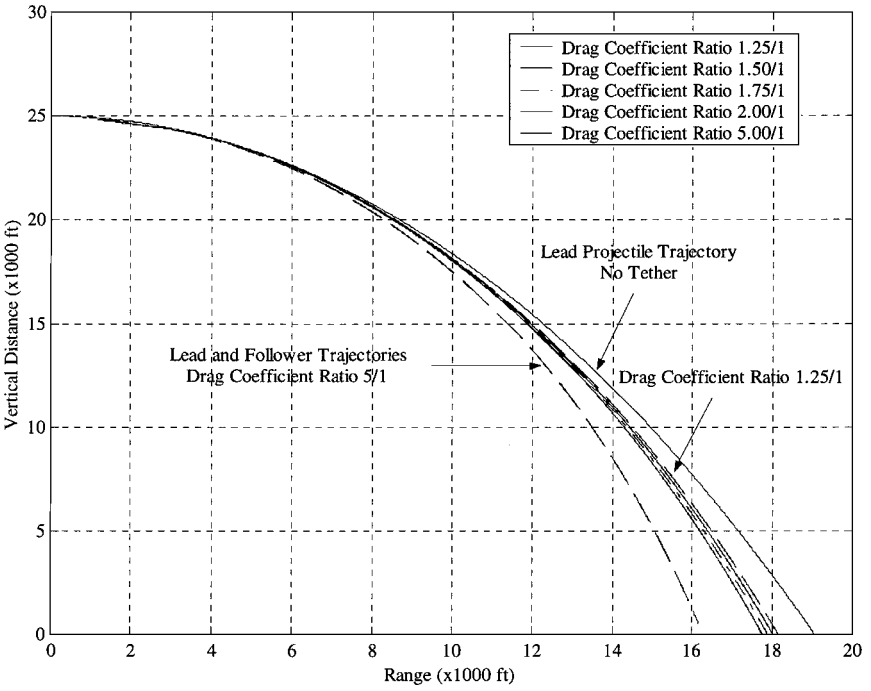

Fig. 1 Projectile range vs time (follower/lead projectile mass ratio 1%).

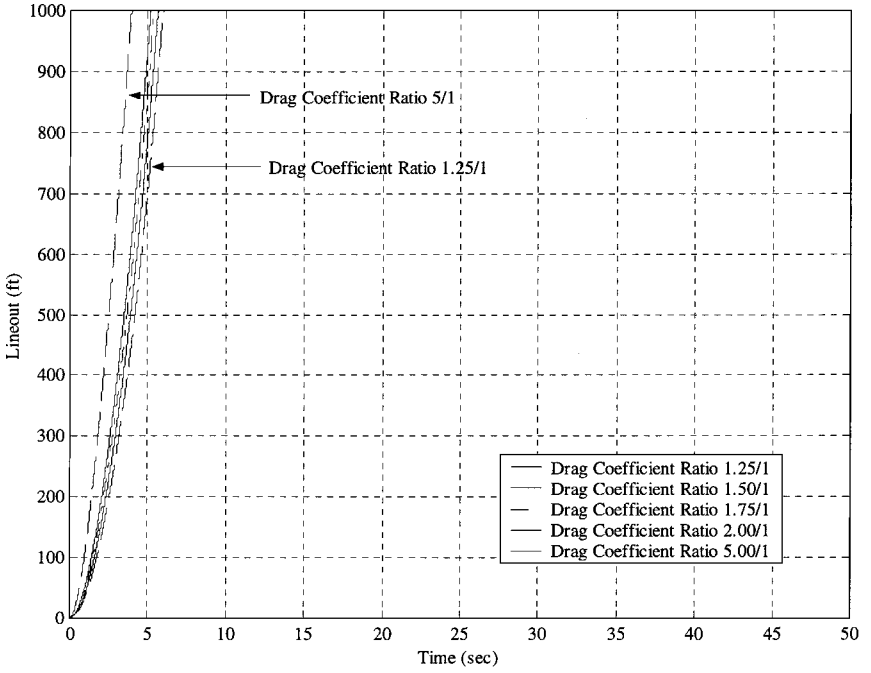

Fig. 2 Tether lineout vs time (follower/lead projectile mass ratio 1%).

to zero. As expected, when the follower projectile drag is increased, the speed of the lead projectile is reduced, and the time duration for the ordnance to reach the ground is increased. Figure 4 shows the speed of the follower projectile over the trajectory for different drag coefficient ratios. All traces show the same basic characteristics. Because the steady-state drop velocity of the follower projectile is lower than the aircraft release speed, the speed of the follower projectile initially decreases. The difference in speed between the lead and follower projectiles pays out the tether line. When the tether line is fully deployed, the tether line grabs the follower projectile and rapidly increases its speed. The follower projectile then rebounds toward the lead projectile so much that the tether line goes slack. With the tether line slack the follower projectile again reduces its speed to seek the steady-state drop velocity. This oscillation continues until a steady-state condition is attained where the speed of the lead and follower projectiles is equal. At the end of the trajectory, the lead projectile impacts the ground, and, shortly after, the tether line goes slack and again the speed of the follower projectile decreases as it approaches the steady-state drop velocity. For drag coefficient ratios of 1.25, 1.5, 1.75, 2.0, and 5.0, the maximum tether line tension is 1776, 1979, 2265, 2552, and 3719 lbf (7900, 8803, 10,075, 11,352, and 16,543 N), respectively. Increasing

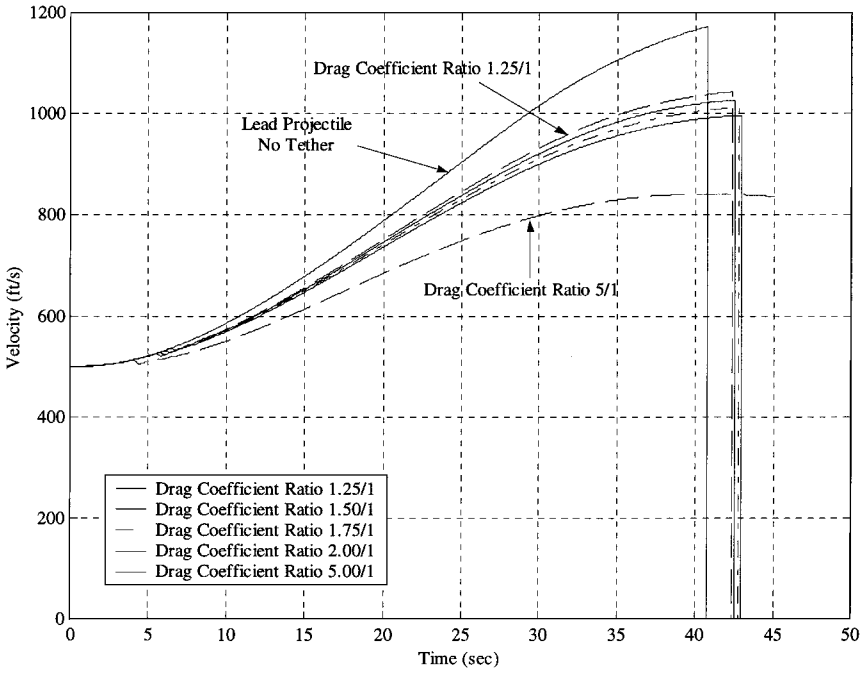

Fig. 3 Lead projectile speed vs time (follower/lead projectile mass ratio 1%).

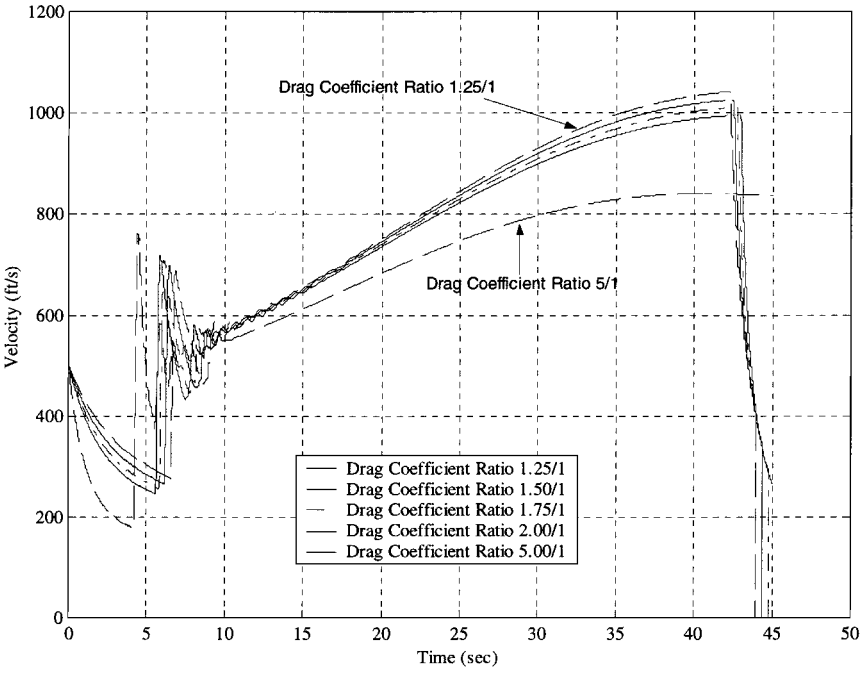

Fig. 4 Follower projectile speed vs time (follower/lead projectile mass ratio 1%).

the drag coefficient ratio steadily increases the maximum instantaneous tether line tension. Designers must take care in selecting the drag coefficient ratio to avoid exceeding the ultimate tether line strength while properly deploying the tether in a specific time interval. The maximum acceleration of the follower projectile also steadily increases with increased drag coefficient ratio. For tether line stiffness of 10,000, 25,000, 50,000, 62,500, and 75,000 lbf-ft/ft (44,482, 111,206, 222,411, 278,013, and 333,616 N-m/m), the maximum tether line tension is 1256, 1700, 2318, 2553, and 2761 lbf (5587, 7562, 10,311, 11,356, 12,282 N), respectively. Increasing the tether line stiffness also steadily increases the maximum instantaneous tether line tension.

Figures 5 and 6 display the speed of the lead and follower projectiles under the same conditions just stated, except the weight of the follower projectile has been increased to 2000 lbf (8896 N) (mass ratio = 100%). As with the 1% mass ratio case just shown, a decrease in range is noticed when the follower projectile drag coefficient is increased. However, for drag coefficient ratios of 1.75 and less, the tether line never becomes fully deployed before the lead projectile contacts the ground. For drag coefficient ratios of 2.0 and 5.0, oscillations from the snatch point do not subside before the lead projectile impacts the ground. Because the tether line for the low drag coefficient ratios is never fully deployed, the lead and follower projectiles approach their steady-state drop velocities with a slack tether line. Unlike the 1% mass ratio case just studied, the lead projectile's speed is greatly affected by the snatch load for the drag coefficient ratio of 5.0. The other traces do not exhibit this characteristic because the snatch point does not occur or occurs just prior to the lead projectile impacting the ground. Also, the lead and follower projectiles never approach a steady-state condition.

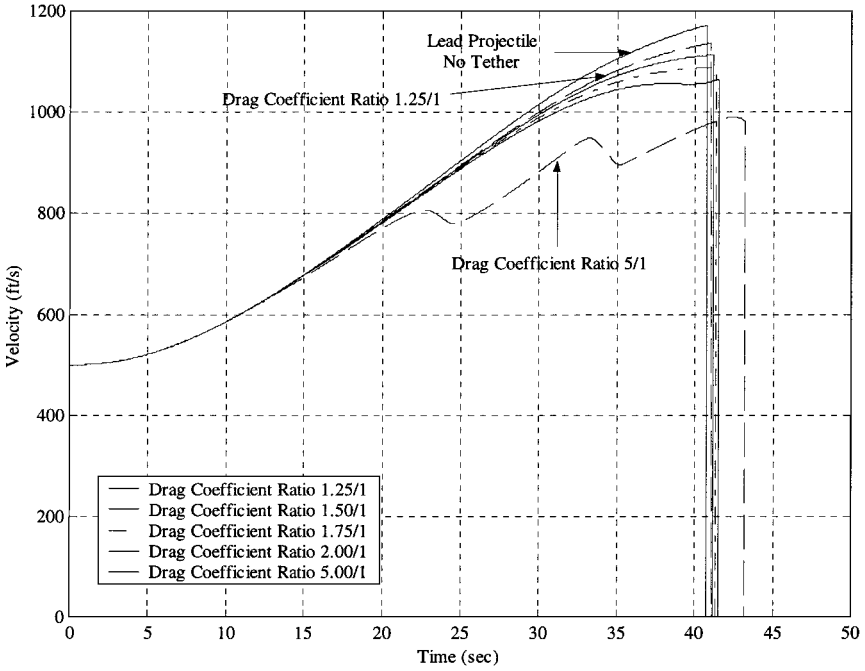

Fig. 5 Lead projectile speed vs time (follower/lead projectile mass ratio 100%).

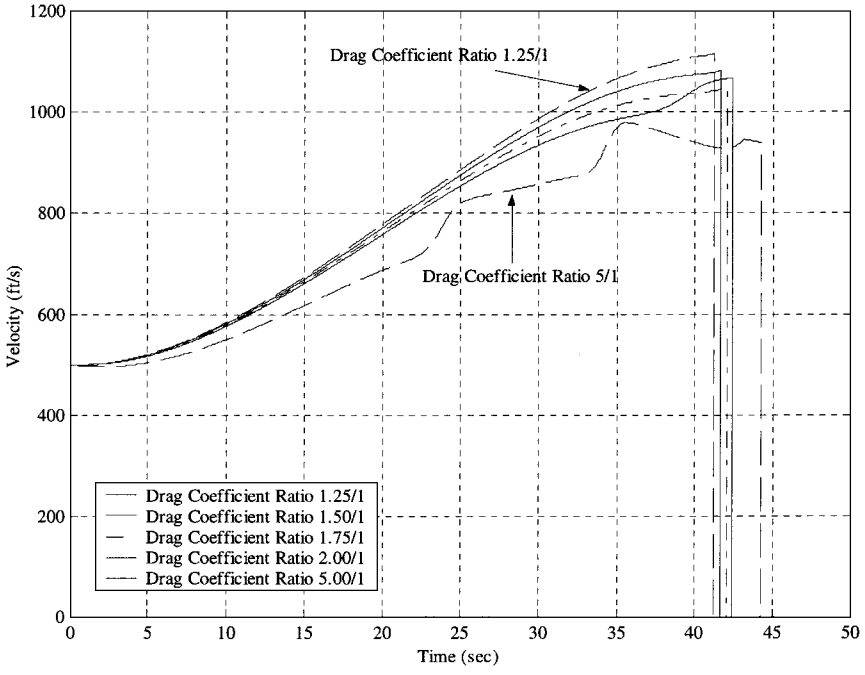

Fig. 6 Lead projectile speed vs time (follower/lead projectile mass ratio 100%).

Conclusions

For a low follower-to-lead-projectile mass ratio, the tether line is unreeled rapidly by the difference in position between the projectiles. For large mass ratios the tether line aerodynamic force unreels the tether line because trajectory differences between the lead and follower projectiles occur relatively slowly. Hence, the tether line unreels itself. Ordnance retrofitted with a tethered sensor will require updated bomb drop schedules because impact points can be altered by up to 15% for high drag coefficient ratio and low mass ratio system configurations. The tether line stiffness has very little effect on the position dynamics but does strongly influence dynamic loading. From a design standpoint a low stiffness, high ultimate strength tether material is most desirable. Proper tether material selection must consider both ultimate line strength and tether stiffness, which both affect loads. For a low mass ratio configuration, an increase in the follower-to-lead-projectile drag coefficient ratio has the expected effect of decreasing tether line deployment time and increasing tether line loads and follower projectile maximum acceleration.

References

[1]Tye, G., and Han, R., "Attitude Dynamics Investigation of the OEDIPUS—A Tethered Rocket Payload," *Journal of Spacecraft and Rockets*, Vol. 32, No. 1, 1995, pp. 133–141.

[2]Puig-Suari, J., Longuski, J., and Tragesser, S., "Aerocapture with a Flexible Tether," *Journal of Guidance, Control, and Dynamics*, Vol. 18, No. 6, 1995, pp. 1305–1312.

[3]No, T. S., and Cochran, J. E., "Dynamics and Control of a Tethered Flight Vehicle," *Journal of Guidance, Control, and Dynamics*, Vol. 18, No. 1, 1995, pp. 2411–2429.

[4]Clifton, J. M., Schmidt, L. V., and Stuart, T. D., "Dynamic Modeling

of a Trailing Wire Towed by an Orbiting Aircraft," *Journal of Guidance, Control, and Dynamics*, Vol. 18, No. 4, 1995, pp. 875–881.

[5]Doyle, G. R., Jr., "Mathematical Model for the Ascent and Descent of a High-Altitude Tethered Balloon," *Journal of Aircraft*, Vol. 6, No. 5, 1969, pp. 457–462.

[6]Matthews, W., "Camera May Relay Instant Images of Bomb Damage," *Air Force Times*, Vol. 58, No. 1, 1997, p. 13.

[7]Frost, G., and Costello, M., "Improved Deployment Characteristics of a Tether Connected Munition System," *Journal of Guidance, Control, and Dynamics*, (to be published).

[8]Von Mises, R., *Theory of Flight*, Dover, New York, 1959, pp. 8–13, Chap. 1.

New Method for Extracting the Quaternion from a Rotation Matrix

Itzhack Y. Bar-Itzhack*
Technion—Israel Institute of Technology, 32000 Haifa, Israel

Introduction

ATTITUDE can be represented in several ways. Because the representations are of the same attitude, there must be a relationship between the different representations, and it must be possible to pass from one to another. The most popular representations of attitude are the direction cosine matrix (DCM) and the quaternion of rotation. Whereas the passage from the quaternion to the corresponding DCM is unique and straightforward, the passage from the DCM to the quaternion is not. Indeed, several algorithms were presented in the literature for computing the quaternion from the corresponding DCM[1–3]; all are based on the solution of nonlinear algebraic equations where the unknowns are the quaternion components and the knowns are the DCM elements. As noted by Shepperd,[3] Grubin's algorithm[1] degrades for large rotations and suffers from singularity when applied to a DCM that represents a 180-deg rotation. On the other hand, Klumpp's algorithm[2] is free of this singularity, but at the expense of the computation of four square roots that requires a cumbersome logic to determine the sign of the computed quaternion elements. At the present, Shepperd's algorithm or variants thereof are the simplest and most popular algorithms, but they require a square root computation and a certain voting in the way the quaternion elements are computed.

In this Note we suggest an algorithm, for extracting the quaternion from the corresponding DCM, which is valid for all attitudes and does not require any voting. Moreover, if the given DCM is not precise and, thereby, is not orthogonal, it yields the optimal quaternion in the sense that it is the quaternion that corresponds to the orthogonal matrix closest to the given imprecise DCM. The algorithm is particularly useful to users of QUEST[4] or who solve the q method directly using an algorithm that computes matrix eigenvalues and eigenvectors.

New Algorithm

In contrast to the three algorithms mentioned before that were based on the solution of nonlinear algebraic equations, the new algorithm is based on the q method.[5] The development of the new algorithm is presented in the following sections. In this section we describe the algorithm itself. The algorithm has three versions depending on the given DCM. The first two algorithms are for a given orthogonal attitude matrix.

Received 29 November 1999; revision received 19 April 2000; accepted for publication 31 July 2000.

*Sophie and William Shamban Professor of Aerospace Engineering, Member Technion Asher Space Research Institute; ibaritz@techunix.technion.ac.il. Fellow AIAA.

Version 1

1) Given an orthogonal 3×3 matrix D, form a matrix K_2 as follows:

$$K_2 = \frac{1}{2}\begin{bmatrix} d_{11}-d_{22} & d_{21}+d_{12} & d_{31} & -d_{32} \\ d_{21}+d_{12} & d_{22}-d_{11} & d_{32} & d_{31} \\ d_{31} & d_{32} & -d_{11}-d_{22} & d_{12}-d_{21} \\ -d_{32} & d_{31} & d_{12}-d_{21} & d_{11}+d_{22} \end{bmatrix} \tag{1}$$

2) Compute the eigenvector of K_2 that belongs to the eigenvalue 1. This is the sought quaternion of D.

Version 2

1) Given an orthogonal 3×3 matrix D, form a K_3 matrix as follows:

$$K_3 = \frac{1}{3}\begin{bmatrix} d_{11}-d_{22}-d_{33} & d_{21}+d_{12} & d_{31}+d_{13} & d_{23}-d_{32} \\ d_{21}+d_{12} & d_{22}-d_{11}-d_{33} & d_{32}+d_{23} & d_{31}-d_{13} \\ d_{31}+d_{13} & d_{32}+d_{23} & d_{33}-d_{11}-d_{22} & d_{12}-d_{21} \\ d_{23}-d_{32} & d_{31}-d_{13} & d_{12}-d_{21} & d_{11}+d_{22}+d_{33} \end{bmatrix} \tag{2}$$

2) Compute the eigenvector of K_3 that belongs to the eigenvalue 1. This is the sought quaternion of D.

Version 3

1) Given a nonorthogonal 3×3 matrix D, form the K_3 matrix as in Eq. (2).

2) Compute the eigenvalues of K_3.

3) Choose $\lambda_{\max}$, the largest eigenvalue of K_3.

4) Compute the eigenvector of K_3 that corresponds to the eigenvalue $\lambda_{\max}$.

This is the sought quaternion of D.

The new algorithm is based on Davenport's q method (see Refs. 5 and 6); therefore, we start our presentation of the algorithm by a short description of this method.

q Method

In 1965, Wahba[7] posed the following problem. Given are k abstract unit vectors that are resolved in a reference and in body Cartesian coordinates. Resolved in the reference coordinates, these unit vectors are denoted by $\boldsymbol{r}_i$, $i = 1, 2, \ldots, k$, and in the body coordinates they are denoted by $\boldsymbol{b}_i$, $i = 1, 2, \ldots, k$. Find the orthogonal 3×3 matrix D that minimizes the cost function L given by

$$L(D) = \frac{1}{2}\sum_{i=1}^{k} a_i |\boldsymbol{b}_i - D\boldsymbol{r}_i|^2 \tag{3}$$

where a_i is a weight we assign to the ith pair. We may want to find the quaternion rather than the matrix representation of attitude. In such a case, Eq. (3) is replaced by

$$J(\boldsymbol{q}) = \frac{1}{2}\sum_{i=1}^{k} a_i |\boldsymbol{b}_i - D(\boldsymbol{q})\boldsymbol{r}_i|^2 \tag{4}$$

In Eq. (4), we are looking for that quaternion $\boldsymbol{q}$ of unit length that minimizes J. As explained by Keat,[5] Davenport showed that the sought $\boldsymbol{q}$ is the eigenvector that corresponds to the largest eigenvalue of a certain matrix K, which is constructed as follows.

Define σ, B, S, and z

$$\sigma = \sum_{i=1}^{k} a_i \boldsymbol{b}_i^T \boldsymbol{r}_i \tag{5a}$$

$$B = \sum_{i=1}^{k} a_i \boldsymbol{b}_i \boldsymbol{r}_i^T \tag{5b}$$

$$S = B + B^T \tag{5c}$$

$$z = \sum_{i=1}^{k} a_i \boldsymbol{b}_i \times \boldsymbol{r}_i \tag{5d}$$